Modified from the paper in Algebraic and Geometric Topology 8 (2008) 1223–1247.

All 2-dimensional links in 4-space live inside a universal 3-dimensional polyhedron

C Kearton
V Kurlin

The hexabasic book is the cone of the 1-dimensional skeleton of the union of two tetrahedra glued along a common face. The universal 3-dimensional polyhedron UP is the product of a segment and the hexabasic book. We show that any closed 2-dimensional surface in 4-space is isotopic to a surface in UP. The proof is based on a representation of surfaces in 4-space by marked graphs, links with double intersections in 3-space. We construct a finitely presented semigroup whose central elements uniquely encode all isotopy classes of 2-dimensional surfaces.

57Q45; 57Q35, 57Q37

1 Introduction

1.1 Brief summary

This is a research on the interface between geometric topology, singularity theory and semigroups. A 2-link is a closed 2-dimensional surface in 4-dimensional space $\mathbb{R}^4$. We study 2-links up to isotopy that is a smooth deformation of the ambient 4-dimensional space. We prove that any 2-link is isotopic to a surface embedded into the universal 3-dimensional polyhedron UP. We also reduce the isotopy classification of 2-links in 4-space to a word problem in a finitely presented semigroup.

1.2 The universal polyhedron containing 2-dimensional links

First we define the universal 3-dimensional polyhedron UP.

Definition 1.1 The *theta* graph TG consists of 3 edges connecting 2 vertices. The *circled* theta graph CT is $\mathrm{TG} \cup S^1$, where the circle S^1 meets each edge of TG in one point, see Fig. 1. Then CT is the 1-dimensional skeleton of two tetrahedra glued along a common face. The *hexabasic book* HB is the cone of CT. Being embedded in 3-space, the book HB divides a neighbourhood of the central vertex into 6 parts. The *universal* 3-dimensional polyhedron is $\mathrm{UP} = \mathrm{HB} \times [-1,1]$.

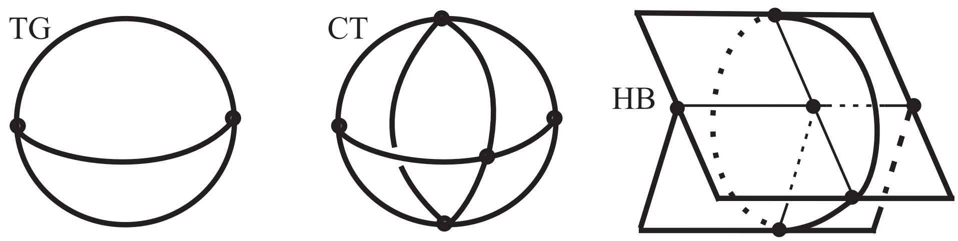

Figure 1: The theta graph TG, circled theta graph CT, book HB

We will work in the smooth category, i.e. all diffeomorphisms are C^∞-smooth. We will make necessary comments on similar constructions in the PL case.

Definition 1.2 An *embedding* is a diffeomorphism onto its image. A *2-link* is a closed (possibly disconnected or non-orientable) smooth surface S embedded into $\mathbb{R}^4$. An *isotopy* between 2-links S and S' is a smooth family of diffeomorphisms $F^u\colon \mathbb{R}^4 \to \mathbb{R}^4$, $u \in [0,1]$, such that $F^0 = \mathrm{id}_{\mathbb{R}^4}$, $F^1(S) = S'$.

Fix the 4th coordinate t in 4-space $\mathbb{R}^3 \times \mathbb{R}$. Then a 2-link in $\mathbb{R}^3 \times \mathbb{R}$ can be studied in terms of its *cross-sections* $S_t = S \cap (\mathbb{R}^3 \times \{t\})$, see Fox and Milnor [7]. Any 2-link can be isotopically deformed to a surface $S \subset \mathbb{R}^3 \times [-1,1]$ such that the projection $\mathrm{pr}\colon S \to [-1,1]$ has distinct non-degenerate critical values. A general cross-section S_t is a classical link in $\mathbb{R}^3 \times \{t\}$, while a cross-section containing a saddle is a link with a double point. When t passes through a saddle, the cross-section $S_t = S \cap (\mathbb{R}^3 \times \{t\})$ changes by the Morse modification in the left picture of Fig. 2.

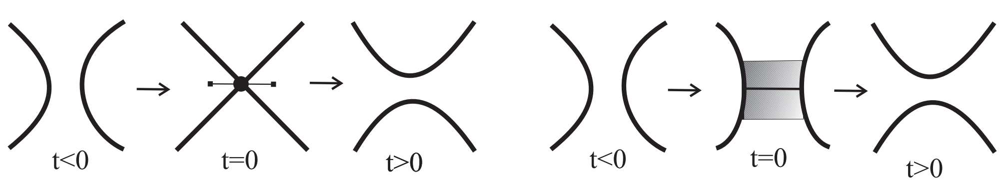

Figure 2: Resolving a singular point and a band in $\mathbb{R}^3$

A PL analogue of the smooth approach is to decompose a 2-link $S \subset \mathbb{R}^3 \times [-1,1]$ into handles located in different sections $\mathbb{R}^3 \times \{t_j\}$. The 1-handles of S will be represented by bands that have a distinguished core and are attached to a classical link in 3-space. Any attached band can be retracted to a singular point marked by a bridge encoding the core of the band. The cross-sections of S below and above every 1-handle locally look like the right picture of Fig. 2.

1.3 Main results

The hexabasic book HB is closely related to the *3-page book* TB, the cone of the *theta* graph TG consisting of 3 edges connecting 2 vertices, see Fig. 7. The *binding* segment of TB is the cone of the 2 vertices of TG. From another point of view, the 3-page book TB can be considered as $\mathbb{R}\times T$, where T is the *triod* consisting of 3 edges connecting the central vertex O to other 3 vertices, here the binding axis α is $\mathbb{R}\times O$. The hexabasic book HB is obtained from TB by adding 3 half-disks whose 6 boundary radii are attached to the 3 edges of $\{0\}\times T$, see Fig. 1.

Theorem 1.3 *Any 2-dimensional link $S\subset\mathbb{R}^4$ is isotopic to a surface embedded into the universal 3-dimensional polyhedron* $\mathrm{UP}=\mathrm{HB}\times[-1,1]$.

The key idea of Theorem 1.3 is to put a given surface S in general position and consider its cross-sections S_t through saddles of $\mathrm{pr}\colon S\to[-1,1]$, see Claim 2.3. Such a cross-section S_t is a link with exactly one singular point, so S_t can be embedded into the 3-page book TB using the technique of 3-page embeddings developed by Kurlin and Vershinin [12, 13], see Proposition 3.2. Both resolutions of the singular point of S_t can be realised in TB, i.e. the embedding extends to a regular neighbourhood of S_t in S. It remains to embed the complement of the regular neighbourhoods of all saddles into $\mathrm{HB}\times[-1,1]$ realising any isotopy of classical links in HB, see Lemma 3.4.

We will develop a 1-dimensional calculus for 2-links as follows. Any 2-link S in general position in $\mathbb{R}^3\times[-1,1]$ can be represented by a banded link BL whose bands are associated to the saddles of $\mathrm{pr}\colon S\to[-1,1]$, see Proposition 2.6(i). Retracting each band to a point, we get a marked graph whose singular points are marked by bridges encoding the cores of bands. There is a complete set of moves on marked graphs generating any isotopy of 2-links in 4-space, see Proposition 4.1. Any marked graph can be embedded into the 3-page book TB and can be encoded by a word in the alphabet of 15 letters. The moves on marked graphs are translated into relations on words, which leads to the universal semigroup SL of 2-links in 4-space.

Introduce the universal semigroup SL generated by the letters a_i,b_i,c_i,d_i,x_i subject to relations (1–1)-(1–8), where $i\in\mathbb{Z}_3=\{0,1,2\}$, e.g. $0-1=2\pmod 3$.

(1–1) $$d_0d_1d_2 = 1, \quad b_id_i = 1 = d_ib_i$$

(1–2) $$a_i = a_{i+1}d_{i-1}, \quad b_i = a_{i-1}c_{i+1}, \quad c_i = b_{i-1}c_{i+1}, \quad d_i = a_{i+1}c_{i-1}$$

(1–3) $$uv = vu, u \in \{a_ib_i, d_ic_i, b_{i-1}d_id_{i-1}b_i, d_ix_ib_i\}, v \in \{a_{i+1}, b_{i+1}, c_{i+1}, b_id_{i+1}d_i, x_{i+1}\}$$

(1–4) $$x_{i-1} = b_{i+1}x_id_{i+1}, \quad b_ix_ib_i = a_i(b_ix_ib_i)c_i, \quad d_ix_id_i = a_i(d_ix_id_i)c_i$$

(1–5) $$(d_ix_ib_i)d_i^2d_{i+1}^2d_{i-1}^2 = d_i^2d_{i+1}^2d_{i-1}^2(d_ix_ib_i)$$

(1–6) $$a_ix_i = a_i, \quad a_ib_ix_id_ic_i = 1$$

(1–7) $$d_ix_ib_ic_ix_i = b_ix_id_ic_ix_i$$

(1–8) $$w_id_{i+1}d_i^2d_{i-1}a_{i+1}b_{i+1}x_ib_id_{i+1}b_i^2b_{i+1}d_i^2 = w_ib_{i-1}b_ia_ib_{i+1}a_{i+1}d_i^2c_{i-1}b_ix_ib_i, \text{ where } w_i = a_ib_ix_ib_ic_i$$

One of the 6 relations $b_id_i = 1 = d_ib_i$ is superfluous and can be deduced from the remaining relations in (1–1). Moreover, the commutativity of d_ic_i with a_{i+1}, b_{i+1} follows from the other relations in (1–3), see more details in Kurlin [12]. So the semigroup SL is generated by not more than 15 letters and 96 relations.

Theorem 1.4 *Any 2-link $S \subset \mathbb{R}^4$ is encoded by an element $w_S \in \mathrm{SL}$ in such a way that 2-links S, S' are isotopic if and only if their encoding elements w_S and $w_{S'}$ are equal in* SL. *An element $w \in \mathrm{SL}$ encodes a 2-link if and only if w is central in* SL.

Outline. In section 2 one represents 2-links in 4-space by banded links and marked graphs in 3-space. Theorems 1.3 and 1.4 are proved in sections 3 and 4, respectively. Banded links are more convenient for deriving a complete set of moves generating any isotopy of 2-links. Marked graphs will be used to prove our main results on embedding and encoding 2-links up to isotopy.

1.4 Acknowledgements

The authors thank S Carter, F Tari and the anonymous referee for useful suggestions.

2 Representing 2-links by banded links and marked graphs

2.1 Critical level embeddings of 2-links in 4-space

Here we describe the PL approach where a 2-link is isotopically deformed to a nice embedding with handles at different levels. The smooth version of crucial Claim 2.3(ii) is a standard statement on general position proved in section 5.

Definition 2.1 A *handle* of dimension n and index k is $D^k \times D^{n-k}$. A *handle decomposition* of a manifold M^n is a sequence of submanifolds $M_0 \subset M_1 \subset \cdots \subset M_l = M$, where M_0 is a disjoint union of n-dimensional disks, each M_{i+1} is obtained from M_i by adding a handle of some index k_i. One can write $M_{i+1} = M_i \cup_{\varphi_i} (D^{k_i} \times D^{n-k_i})$, where $\varphi_i : \partial D^{k_i} \times D^{n-k_i} \to \partial M_i$ is an embedding. If before and after each handle addition one inserts a *collar*, the product of the attaching area and a segment, then one gets a *collared handle* decomposition, see Kearton and Lickorish [11, p. 416].

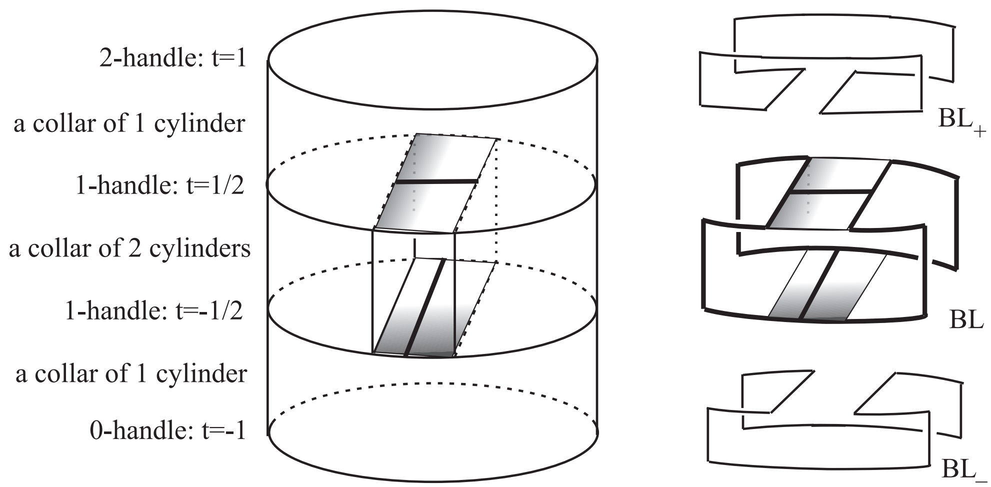

Figure 3: A critical level embedded torus and its banded link $BL \subset \mathbb{R}^3$

A 2-link with a collared handle decomposition can be nicely embedded in $\mathbb{R}^4$. The left picture of Fig. 3 shows a similar embedding, where the standard 2-torus in $\mathbb{R}^3$ has the collared handle decomposition consisting of 4 handles and 3 collars:

1) the lowest handle is a 0-handle (a disk) at the level $t = -1$;

2) the 2 intermediate handles are 1-handles (bands) at the levels $t = \pm 1/2$;

3) the highest handle is a 2-handle (a disk) at the level $t = +1$.

Definition 2.2 A *critical level* PL embedding is a PL embedding of a 2-link $S \subset \mathbb{R}^3 \times [-1, 1]$ with a collared handle decomposition satisfying (i), (ii), see Kearton and Lickorish [11, p. 417]:

(i) the handles are in different sections $\mathbb{R}^3 \times \{t_j\}$, where $-1 < t_1 < \cdots < t_n < 1$;

(ii) each collar between adjacent handles of S is embedded as the direct product $A \times [t_j, t_{j+1}] \subset \mathbb{R}^3 \times [t_j, t_{j+1}]$, where $A \subset \mathbb{R}^3$ is the attaching area of the handles.

A smooth embedding $S \subset \mathbb{R}^3 \times [-1, 1]$ is called a smooth *critical level* embedding if the projection $\mathrm{pr}\colon S \to [-1, 1]$ has all its critical points in different sections $\mathbb{R}^3 \times \{t_j\}$. This is a general position assumption.

Claim 2.3 *(i) (Kearton and Lickorish [11, Theorem 1, p. 420]) Any 2-dimensional PL link in 4-space is isotopic to the image of a critical level PL embedding $S \subset \mathbb{R}^3 \times [-1, 1]$.*

(ii) Any smooth 2-link is smoothly isotopic to a surface $S \subset \mathbb{R}^3 \times [-1, 1]$ such that all critical points of $\mathrm{pr}\colon S \to [-1, 1]$ are non-degenerate and have distinct values.

We will use the smooth version of Claim 2.3(ii), which will be deduced from the transversality theorem of Thom in section 5. Claim 2.3(i) is worth keeping in mind when one associates a banded link to a 2-link in Proposition 2.6(i).

2.2 Representing 2-links in 4-space by banded links in 3-space

We define banded links, links with bands, which will represent 2-links in 4-space.

Definition 2.4 A *banded* link is a collection of circles and bands in $\mathbb{R}^3$ such that

(i) the circles and bands are non-oriented and non-self-intersecting;

(ii) the circles and bands are disjoint except for each band having a pair of opposite sides *attached* to disjoint arcs in the circles, the other sides are called *free*.

In every band we mark its *core*, an arc connecting its attached opposite sides, see Fig. 3. Banded links are considered up to isotopy of $\mathbb{R}^3$. The bands of a banded link will represent 1-handles of a 2-link. In every band B of a banded link BL consider the opposite free sides not connected by the core of B. Replace B by its free sides, the resulting usual non-oriented link in $\mathbb{R}^3$ is called the *positive* resolution BL_+ of the banded link BL, see the right picture of Fig. 3. Similarly define the *negative* resolution BL_- replacing every band B by the opposite attached sides connected by the core of B. A banded link BL is *admissible*, if both resolutions $BL_\pm$ are trivial links.

If a PL 2-link $S \subset \mathbb{R}^3 \times [-1,1]$ has all its 1-handles in the zero section $\mathbb{R}^3 \times \{t=0\}$, then the cross-section $S_0 = S \cap (\mathbb{R}^3 \times \{t=0\})$ is a banded link. We will use much weaker assumptions and construct a banded link for any critical level embedding. Proposition 2.6 leads to a calculus for 2-links in Proposition 4.1 and provides a function from the set of 2-links to the set of admissible banded links.

Definition 2.5 Given a 2-dimensional surface S, consider the space of all smooth functions $f\colon S \to \mathbb{R}^4$ with the Whitney topology, see Definition 5.2. The space CS of all 2-links $S \subset \mathbb{R}^4$ has the induced topology. Points in CS will be classified using the projection $\mathrm{pr}\colon S \to \mathbb{R}$ to the 4th coordinate t. A 2-link $S \in \mathrm{CS}$ is called

- *generic* if all critical points of pr are non-degenerate and have distinct values;
- an $A_1^+A_1^+$-*singularity* if S fails to be generic because of 2 non-degenerate extrema of $\mathrm{pr}\colon S \to \mathbb{R}$ that have the same value;
- an $A_1^+A_1^-$ -*singularity* if S fails to be generic because of a non-degenerate saddle and extremum of $\mathrm{pr}\colon S \to \mathbb{R}$ that have the same value;
- an $A_1^-A_1^-$ -*singularity* if S fails to be generic because of 2 non-degenerate saddles of $\mathrm{pr}\colon S \to \mathbb{R}$ that have the same value;
- an A_2-*singularity* if S fails to be generic because of a singularity of $\mathrm{pr}\colon S \to \mathbb{R}$ having the form $\mathrm{pr}(x,y) = x^2 - y^3$ in local coordinates x,y.

The sign in the notation above is the sign of the determinant $\mathrm{pr}_{xx}\mathrm{pr}_{yy} - \mathrm{pr}_{xy}^2$ of the Jacobi matrix of 2nd order derivatives at a critical point. Denote by $\Sigma_{++}, \Sigma_{+-}, \Sigma_{--}$ and Σ_2 the *subspaces* of the corresponding singularities in the space CS. Introduce the *singular* subspace $\Sigma = \Sigma_{++} \cup \Sigma_{+-} \cup \Sigma_{--} \cup \Sigma_2$. An isotopy of 2-links can be considered as a path in CS. In Proposition 2.6 we consider paths nicely meeting the singular subspace Σ.

Proposition 2.6 *(i) To any a critical level embedding $S \subset \mathbb{R}^3 \times [-1,1]$ we associate a banded link BL well-defined up to the slide/swim moves in Fig. 4.*

(ii) If 2-links S, S' are isotopic through generic 2-links, then the associated banded links BL, BL' are related by the slide/swim moves in Fig. 4.

(iii) If 2-links S, S' are isotopic through generic 2-links and one of $A_1^+A_1^+, A_1^+A_1^-, A_1^-A_1^-$ -singularities, then BL, BL' are related by the slide/swim moves in Fig. 4.

(iv) If 2-links S, S' are isotopic through generic 2-links and exactly one A_2-singularity, then BL, BL' are related by the cap/cup and slide/swim moves in Fig. 4.

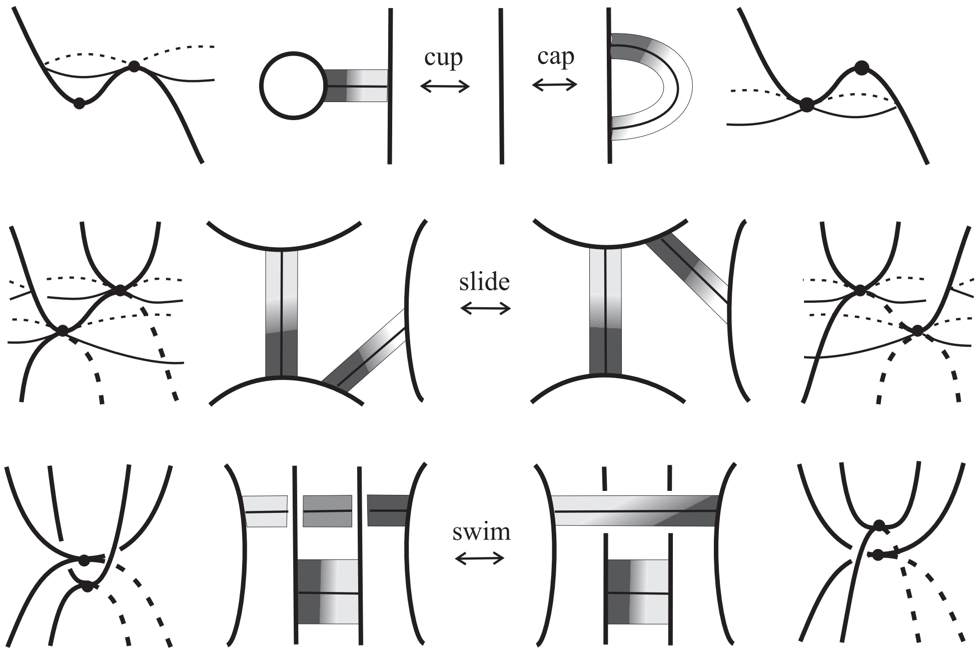

Figure 4: Cup/cap moves and slide/swim moves of banded links

Proof (i) The lowest critical point of a generic 2-link S with respect to $\mathrm{pr} : S \to [-1,1]$ at $t = t_1$ is a minimum, so the cross-section $S_{t_1+\varepsilon}$ is a trivial knot for some $\varepsilon > 0$. The section $S_{t_1+\varepsilon}$ is a prototype of a future banded link BL, which will be located in a fixed copy of $\mathbb{R}^3$. The key idea in constructing BL is to watch the current cross-section $S_t = S \cap (\mathbb{R}^3 \times \{t\})$ simultaneously adding bands and trivial knots corresponding to new saddles and minima, respectively. The left column of Fig. 5 contains cross-sections S_t for different values of t. The right column shows successive stages of constructing BL whose final form is the top right.

While t is increasing, we isotopically deform the current banded link $BL \subset \mathbb{R}^3$ following $S_t = S \cap (\mathbb{R}^3 \times \{t\})$, see Fig. 5. The existing bands of BL can be deformed to avoid intersections with the rest of BL. For each new minimum of S in $\mathbb{R} \times \{t_j\}$, add a trivial knot from $S_{t_j+\varepsilon}$ to the current banded link $BL \subset \mathbb{R}^3$.

For each new saddle of S, attach a small band B to BL. The band B has 2 opposite sides attached to branches of the previous link BL. While t passes the critical value, the attached sides of B are retracted to a point and are replaced by the free sides of B. The band B can not meet the attached sides of other bands of BL since these sides are not included into the current cross-section of S. So there are only 2 cases when the

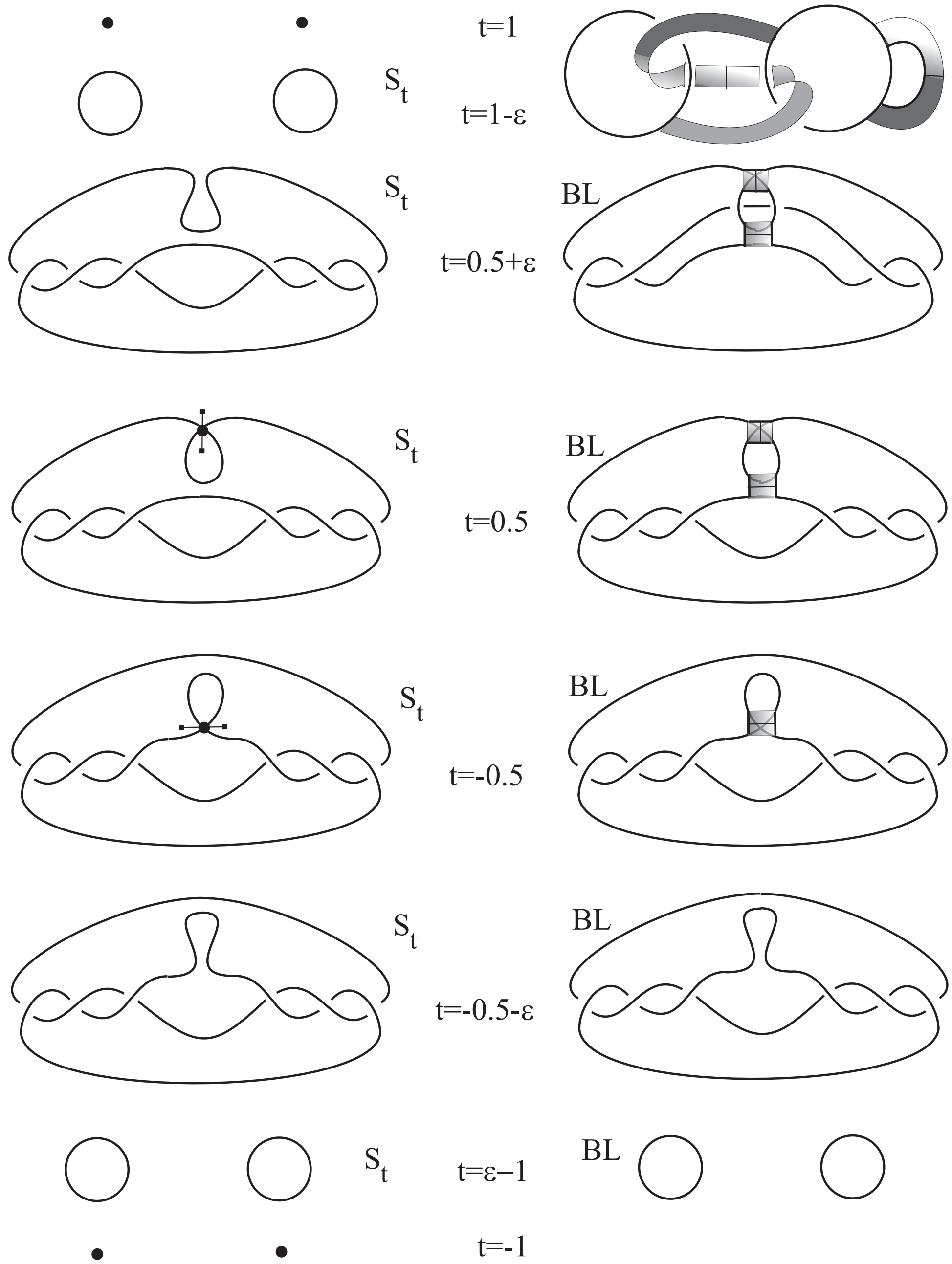

Figure 5: Cross-sections and a banded link of the spun 2-knot of the trefoil

new link with bands does not satisfy Definition 2.4.

(a) One (or two) of the attached sides of B may meet a free side of another band B' of BL, see the upper picture of Fig. 6. Then slide B along the free side of B' in any of the two directions so that in the end the attached side of B does not meet B'.

(b) The band B intersects the interior of another band B' of BL, see the lower picture of Fig. 6. Then B swims through any of the attached sides of B', so B, B' fall apart. The band B can not swim through the free sides of B' as they belong to the current cross-section of S. For each new 2-handle (a maximum), we keep the corresponding trivial knot of BL, although it disappears from $S_t = S \cap (\mathbb{R}^3 \times \{t\})$.

After we have passed all critical values of $\mathrm{pr}\colon S \to \mathbb{R}$, the associated banded link $BL \subset \mathbb{R}^3$ has been constructed.

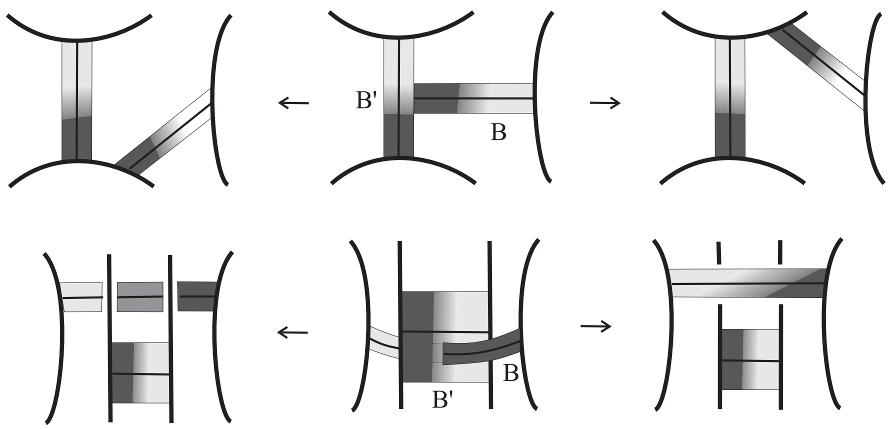

Figure 6: A band slides or swims to remove an intersection

(ii) The construction above is not affected by an isotopy of S keeping the order of critical points of $\mathrm{pr}\colon S \to [-1,1]$. Indeed all cross-sections S_t are replaced by isotopic links, so the resulting banded link is isotopic to the original one provided that we remove intersections of bands in Fig. 6 in the same way.

(iii) The given isotopy of S is a smooth path passing through one of $A_1^+A_1^+, A_1^+A_1^-, A_1^-A_1^-$-singularities in the space CS of 2-links. For $A_1^+A_1^+$ or $A_1^+A_1^-$, an extremum and another singularity swap their heights, so we add a new trivial knot (passing a minimum) or keep an existing trivial knot (passing a maximum) that does not affect the other singularity. For an $A_1^-A_1^-$-singularity, two saddles of S swap their heights, so we add

2 bands to *BL* in the reverse order. Consider the critical moment when both saddles are in the same section $\mathbb{R}^3 \times \{t_j\}$. If the associated bands do not intersect each other, then the new banded link is isotopic to the original one. In (i) we listed the only cases (a), (b) when one band may intersect another, which led to the moves in Fig. 6 so the banded links are equivalent through the slide/swim moves.

(iv) If an isotopy of S passes through an A_2-singularity, then around this moment a non-degenerate saddle and extremum appear in a 2-link, see Claim 4.2(iv). In the case of a minimum, one adds a trivial knot to the current banded link *BL* and a band attached to the trivial knot and to an existing branch of *BL* as shown in the cup move of Fig. 4. In the case of a maximum, one adds a band attached by both sides to a branch of the current banded link *BL* as shown in the cap move of Fig. 4. Recall that we keep the trivial knot when t passes a maximum. The leftmost and rightmost columns of Fig. 4 show projections of 2-links to $\mathbb{R}^3$ around singular moments. The 4th axis of $\mathbb{R}^3 \times \mathbb{R}$ projects to the vertical axis of $\mathbb{R}^3$. □

Conversely, any admissible banded link will give rise to a 2-link in 4-space, see Lemma 2.8. One can describe all moves of banded links generating any isotopy of 2-links in 4-space. Banded links were called *knots with bands* in Swenton [14].

2.3 Representing 2-links in 4-space by marked graphs in 3-space

Theorem 1.4 is easier to prove representing 2-links by marked graphs, which are singular links with bridges at singular points.

Definition 2.7 After deformation retracting each band of a banded link *BL* to a point, we get a *singular* link (see Kurlin and Vershinin [13]), a collection of closed curves with finitely many double transversal intersections, see Fig. 2, 5. The core of each retracted band defines a bridge at the singular point, a straight arc in a small plane neighbourhood of each singular point. We consider the resulting *marked* graph *MG* up to isotopy in $\mathbb{R}^3$ keeping a neighbourhood of each singular point in a (moving) plane.

In the smooth approach, the zero section $S \cap (\mathbb{R}^3 \times \{0\})$ containing all saddles of $\mathrm{pr}\colon S \to [-1,1]$ is a marked graph whose bridges show how to resolve the singular points for $t > 0$ (along bridges) and $t < 0$ (across bridges), see Fig. 2, 3. An abstract marked graph *MG*, i.e. a singular link with bridges, can be converted into a banded link *BL* replacing each bridge by a small rectangle whose core coincides with the bridge. So there is a 1-1 correspondence between banded links and marked graphs. Lemma 2.8

provides a unique function from the set of admissible banded links to the set of 2-links, which is the inverse of the function from Proposition 2.6.

Lemma 2.8 *Any admissible banded link $BL \subset \mathbb{R}^3$ gives rise to a 2-link $S \subset \mathbb{R}^4$ that can be represented by BL as in Proposition 2.6(i).*

Proof Take the marked graph $MG \subset \mathbb{R}^3$ associated to the given banded link. Isotopically deform MG in such a way that neighbourhoods of all singular points of MG are contained in a single hyperplane of $\mathbb{R}^3 \times \{0\}$.

Resolving the singular points along the bridges for $t > 0$ and across the bridges for $t < 0$, extend the embedding $MG \subset \mathbb{R}^3 \times \{0\}$ to a surface $S' \subset \mathbb{R}^3 \times [-\varepsilon, \varepsilon]$ for some $\varepsilon > 0$, such that the boundary $\partial S'$ consists of trivial links in $\mathbb{R}^3 \times \{\pm\varepsilon\}$.

Since both sections $S'_{\pm\varepsilon} = S' \cap (\mathbb{R}^3 \times \{t = \pm\varepsilon\})$ are unlinks, one can find isotopies $\varphi_t^{\pm} : \mathbb{R}^3 \to \mathbb{R}^3$, $t \in [\varepsilon, 1-\varepsilon]$, such that each $\varphi_{1-\varepsilon}^{\pm}(S'_{\pm\varepsilon})$ is a collection of small disjoint circles in a plane. The isotopies $\varphi_t^{\pm}$ define the embedding of a 2-link S without small disks into $\mathbb{R}^3 \times [\varepsilon - 1, 1 - \varepsilon]$, one disk for each component of ∂S. Attaching a disc to each boundary circle gives a closed surface $S \subset \mathbb{R}^3 \times [-1, 1]$.

The zero section $S \cap (\mathbb{R}^3 \times \{0\})$ is the original marked graph MG. A small isotopy deformation makes S generic. The construction of Proposition 2.6(i) gives a banded link equivalent to MG as all bands may be chosen small and non-intersecting. □

3 Three-page embeddings of marked graphs

3.1 Any marked graph can be embedded into the 3-page book

Recall that the 3-page book is $\mathrm{TB} = \mathbb{R} \times T$, where T is the triod consisting of 3 edges E_0, E_1, E_2 joining the vertex O to the other 3 vertices. The line $\alpha = \mathbb{R} \times O$ is said to be the *binding* axis, $P_i = \mathbb{R} \times E_i$ are called the *pages*, $i = 0, 1, 2$.

Definition 3.1 An embedding of a marked graph G into the 3-page book TB is called a *3-page* embedding, if conditions (i)-(v) hold:

(i) the intersection $G \cap \alpha$ of G and the binding axis α is a finite set of points;

(ii) the arcs at every point of $G \cap \alpha$ lie in 2 pages P_i, P_j, $i \neq j$, see Fig. 7;

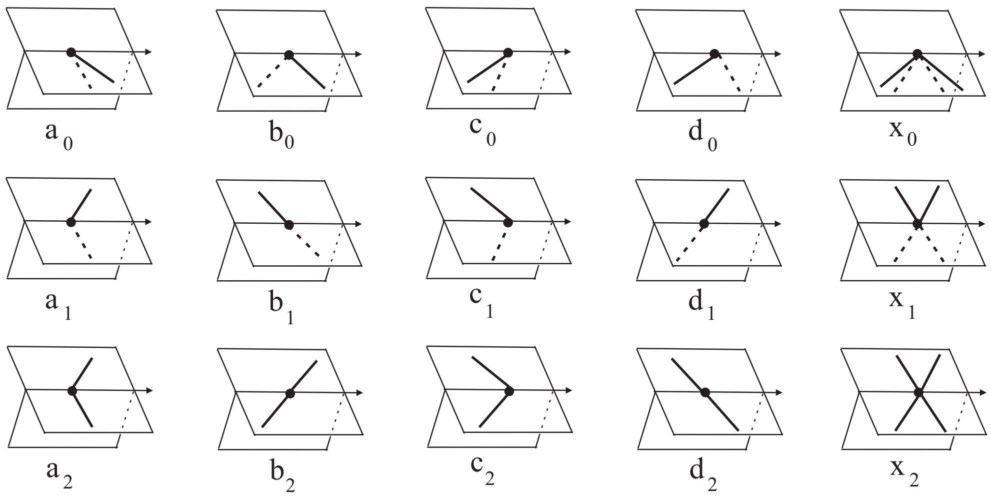

Figure 7: The encoding letters for 3-page embeddings of marked graphs

(iii) all singular points of G lie in α, a neighbourhood of each singular point lies in a broken plane consisting of two pages and looks locally like a cross $\times$;

(iv) the bridge at each singular point lies in the binding axis α;

(v) every connected component of $G \cap P_i$ is projected monotonically to α.

The arcs in the page P_2 are dashed in Fig. 7, 8. All classical and singular links can be embedded into TB in the sense of Definition 3.1, see Fig. 8.

The pictures in each vertical column of Fig. 7 are obtained from each other by rotation around α. The rotation corresponds to the shift $i \mapsto i+1$ of indices, $i \in \mathbb{Z}_3 = \{0,1,2\}$. A 3-page embedding can be encoded by a word in the alphabet of 15 letters describing the local behaviour of G near the intersection points $G \cap \alpha$, see Fig. 7. The 3-page embedding in Fig. 8 is encoded by $w_G = a_0a_1(b_2b_0b_1)^2d_0a_1d_1(x_1b_1)^2c_1d_1b_0(d_1d_0d_2)^2c_1c_0$. So a 3-page embedding of the marked graph G_S of a 2-link S is a 1-dimensional representation of $S \subset \mathbb{R}^4$.

We give a proof of the embedding result from Kurlin and Vershinin [13], because this construction plays an important role in further considerations.

Proposition 3.2 *(Kurlin and Vershinin [13]) Any marked graph $G \subset \mathbb{R}^3$ is isotopic to a 3-page embedding $G \subset$ TB in the sense of Definition 3.1.*

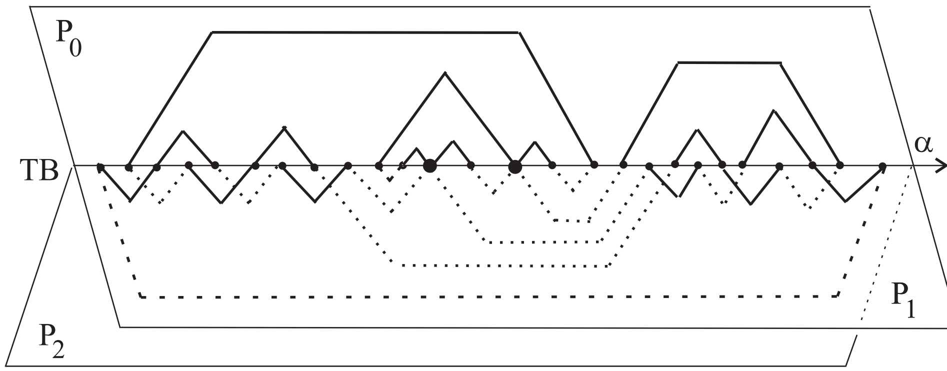

Figure 8: A 3-page embedding of the marked graph from Fig. 9

Proof Consider a plane diagram D of $G \subset \mathbb{R}^3$ in general position with finitely many double crossings. At each crossing in the diagram D mark a small overcrossing arc. Recall that, at each singular point of G, there is a marked bridge transversally intersecting both branches of G passing through the singular point.

In the plane containing the diagram D, draw a continuous path α such that

(1) the path α passes through each marked arc and bridge exactly once;

(2) α transversally intersects the rest of D, the endpoints of α are away from D.

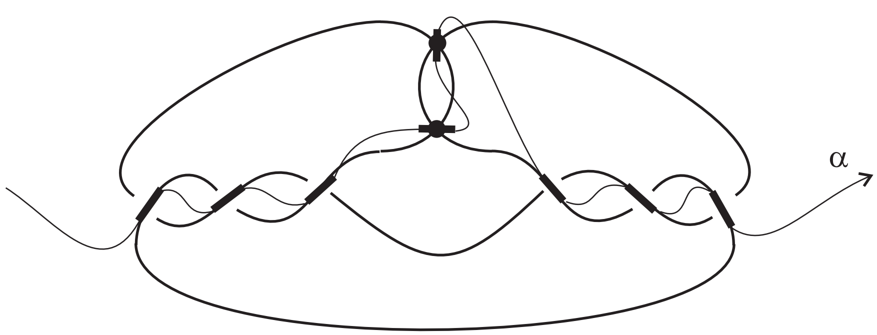

Figure 9: How to construct a 3-page embedding of a marked graph

Isotopically deform the plane containing D in such a way that α becomes a straight line containing all marked arcs and bridges of D. Denote the upper half-plane and lower half-plane of $\mathbb{R}^2 - \alpha$ by P_0 and P_2, respectively. Notice that a neighbourhood of each singular point looks like a cross $\times$ with a centre in the axis α, see Fig. 9.

Attach the third half-plane P_1 to α and push all marked arcs into P_1, see Fig. 8. If both (say) upper arcs at some singular point $v \in G$ go to points on one side of the point $v \in \alpha$, then make an additional couple of crossings in the intersection $\alpha \cap D$ like in Reidemeister move II, see Fig. 13. For instance, in the embedding $a_2 b_2 x_2$ both upper arcs go to the right, see the lower right picture of Fig. 15, more details are in Kurlin and Vershinin [13]. Then the intersection $G \cap P_i$ is a finite collection of disjoint arcs, which can be made monotonic with respect to the projection $\mathrm{TB} \to \alpha$, $i = 0, 1, 2$. □

3.2 Any isotopy of links can be realised in the hexabasic book

The following lemma is a key stone of the 3–page approach to knot theory and was originally proved by I Dynnikov [3, 4].

Lemma 3.3 *(Kurlin [12]) Any isotopy of 3-page embeddings of classical links is decomposed into finitely moves in Fig. 10 and theirs images under* $i \mapsto i+1$, $i \in \mathbb{Z}_3$.

The algebraic form of the moves in Fig. 10 is below, $i \in \mathbb{Z}_3 = \{0, 1, 2\}$, see Kurlin [12]:

(3–1) $$d_0 d_1 d_2 = 1, \quad b_i d_i = 1 = d_i b_i$$

(3–2) $$a_i = a_{i+1} d_{i-1}, \quad b_i = a_{i-1} c_{i+1}, \quad c_i = b_{i-1} c_{i+1}, \quad d_i = a_{i+1} c_{i-1}$$

(3–3) $$uv = vu, \text{ where } u \in \{a_i b_i, d_i c_i, b_{i-1} d_i d_{i-1} b_i\}, v \in \{a_{i+1}, b_{i+1}, c_{i+1}, b_i d_{i+1} d_i\}$$

Lemma 3.4 is the crucial step in Theorem 1.3.

Lemma 3.4 *The moves in Fig. 10 are realised in the hexabasic book* HB.

Proof All the moves in Fig. 10, apart from the commutativity of $a_i, b_i, c_i, b_{i-1} d_i d_{i-1}$ with $b_{i+1} d_{i-1} d_{i+1} b_{i-1}$, can be realised in the 3-page book TB. For instance, the relation $b_2 d_2 = 1$ is realised by compressing the slice between the 2 intersection points and removing the resulting point from α. The other relations are realised in HB, see a geometric realisation of $(b_1 d_2 d_1 b_2) a_0 = a_0 (b_1 d_2 d_1 b_2)$ in Fig. 11. □

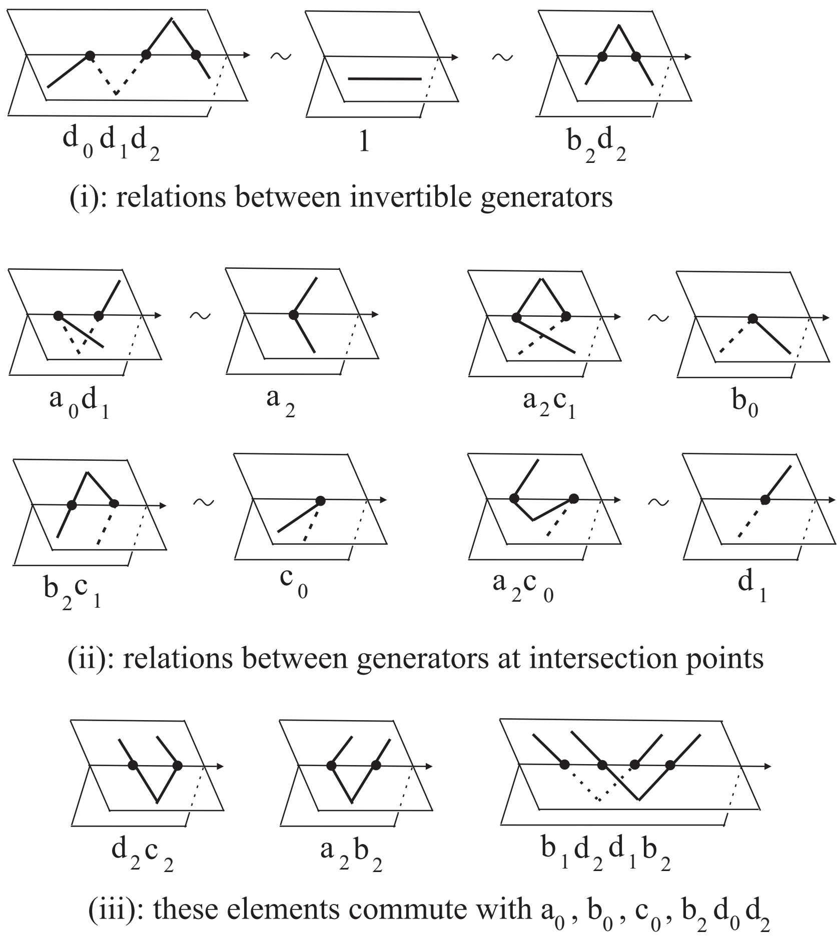

Figure 10: Finitely many moves generating any isotopy of classical links

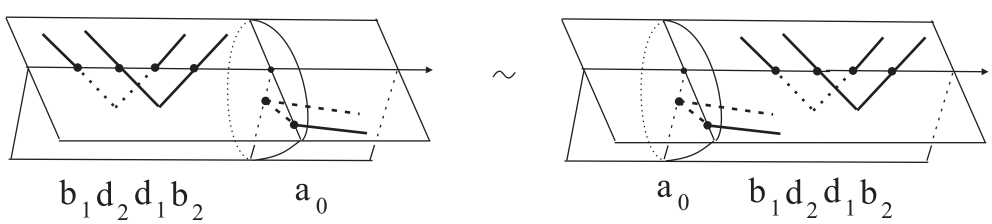

Figure 11: Realising a commutative relation in the hexabasic book HB

3.3 Any 2-link is isotopic to a surface in the universal polyhedron

Here we finish the proof of Theorem 1.3.

Proof of Theorem 1.3 By Claim 2.3 any 2-link in 4-space is isotopic to a surface $S \subset \mathbb{R}^3 \times [-1,1]$ having all maxima, minima and saddles in different sections $\mathbb{R}^3 \times \{t_j\}$ for some $-1 < t_1 < \cdots < t_n < 1$. In Step 1 we embed each cross-section S_{t_j} into the 3-page book. In Step 2 we extend this embedding to a regular neighbourhood of S_{t_j}. In Step 3 we embed the complement of the neighbourhoods into $\mathrm{HB} \times [-1,1]$.

Step 1. Choose $\varepsilon > 0$ such that the closed ε-neighbourhoods $N_\varepsilon(S_{t_j})$ of S_{t_j} in S are disjoint and each of them contains exactly one critical point of $\mathrm{pr} : S \to [-1,1]$, $j = 1, \dots, n$. Then the boundaries $\partial N_\varepsilon(S_{t_j})$ are classical links. By Proposition 3.2 there is an isotopy $f_j^u \colon \mathbb{R}^3 \times \{t_j\} \to \mathbb{R}^3 \times \{t_j\}$, $u \in [0,1]$, moving S_{t_j} into TB, i.e. $f_j^0 = \mathrm{id}_{\mathbb{R}^3}$, $f_j^1(S_{t_j}) \subset \mathrm{TB} \times \{t_j\}$ is a 3-page embedding. Take smooth functions $g_j \colon [t_j - \varepsilon, t_j + \varepsilon] \to [0,1]$ such that $g_j(t_j) = 1$ and $g_j(t_j \pm \varepsilon) = 0$. Extend f_u^j to

$$F_j^u \colon \mathbb{R}^3 \times [t_j - \varepsilon, t_j + \varepsilon] \to \mathbb{R}^3 \times [t_j - \varepsilon, t_j + \varepsilon], \quad u \in [0,1],$$

$$F_j^u(x,t) = (f_j^{ug_j(t)}(x), t), \text{ where } x \in \mathbb{R}^3, t \in [t_j - \varepsilon, t_j + \varepsilon].$$

Then $F_j^u = f_j^u$ for $t = t_j$ and $F_j^u = \mathrm{id}$ for $t = t_j \pm \varepsilon$. Hence $\partial N_\varepsilon(S_{t_j})$ are pointwise fixed and we may combine F_j^u together to form a smooth isotopy $F^u \colon \mathbb{R}^3 \times [-1,1] \to \mathbb{R}^3 \times [-1,1]$ moving each S_{t_j} into $\mathrm{TB} \times \{t_j\}$. Denote the resulting surface by S'.

Step 2. If a singular cross-section S'_{t_j} has a double intersection, then both positive and negative resolutions of S'_{t_j} can be embedded into TB. Indeed the positive and negative resolutions of the singular point x_i are encoded by 1 and $c_i a_i$, respectively, see Fig. 12. Given an encoding word w_j of $S'_{t_j} \subset \mathrm{TB}$, the positive resolution of S'_{t_j} is encoded by w_j after removing the letter x_i representing the double point of S'_{t_j}.

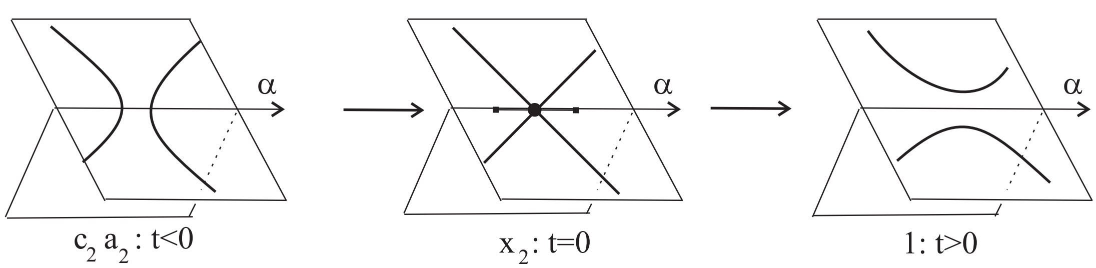

Figure 12: Resolving a singular point in the 3-page book TB

The argument below with the sign $\pm$ covers 2 cases when either $+$ or $-$ is taken in all formulae. If S'_{t_j} contains a maximum or minimum, $S'_{t_j\pm\varepsilon/2}$ can be embedded into TB. So there are isotopies $h^u_{\pm j}\colon \mathbb{R}^3\times\{t_j\pm\varepsilon/2\}\to\mathbb{R}^3\times\{t_j\pm\varepsilon/2\}$, $u\in[0,1]$, moving each $S'_{t_j\pm\varepsilon/2}$ into $\mathrm{TB}\times\{t_j\pm\varepsilon/2\}$. Take smooth functions $\tilde g_j\colon [t_j-\varepsilon,t_j+\varepsilon]\to[0,1]$ such that $\tilde g_j(t_j)=0=\tilde g_j(t_j\pm\varepsilon)$ and $\tilde g_j(t_j\pm\varepsilon/2)=1$. Extend $h^u_{\pm j}$ to

$$H^u_j\colon \mathbb{R}^3\times[t_j-\varepsilon,t_j+\varepsilon]\to\mathbb{R}^3\times[t_j-\varepsilon,t_j+\varepsilon],\quad u\in[0,1],$$

$$H^u_j(x,t)=(h^{u\tilde g_j(t)}_{\pm j}(x),t)\text{ for }x\in\mathbb{R}^3,\ t\text{ between }t_j\text{ and }t_j\pm\varepsilon.$$

Then $H^u_j=h^u_{\pm j}$ for $t=t_j\pm\varepsilon/2$ and $H^u_j=\mathrm{id}$ for $t=t_j$, $t=t_j\pm\varepsilon$. Hence S'_{t_j} and $\partial N_\varepsilon(S'_{t_j})$ are pointwise fixed and we may combine H^u_j together to form a smooth isotopy $H^u\colon \mathbb{R}^3\times[-1,1]\to\mathbb{R}^3\times[-1,1]$ moving each $N_{\varepsilon/2}(S'_{t_j})$ into $\mathrm{TB}\times[t_j-\varepsilon/2,t_j+\varepsilon/2]$. Denote the resulting surface by S''.

Step 3. The cross-sections $S''_{t_j+\varepsilon/2}$ and $S''_{t_{j+1}-\varepsilon/2}$ are isotopic classical links, $j=1,\dots,n-1$. By Lemmas 3.3 and 3.4 any isotopy of classical links can be realised in HB. Then the layers $S''\cap(\mathbb{R}^3\times[t_j+\varepsilon/2,t_{j+1}-\varepsilon/2])$ can be replaced by an isotopy of links in $\mathrm{HB}\times[t_j+\varepsilon/2,t_{j+1}-\varepsilon/2]$. It remains to extend the embedding to the neighbourhoods of the lowest minimum and highest maximum of S'' shrinking their boundaries in HB. So the final surface is embedded into $\mathrm{HB}\times[-1,1]$. □

4 The universal semigroup of 2-dimensional links

4.1 Local moves of marked graphs generate any isotopy of 2-links

Here we derive a complete set of moves of banded links and marked graphs, that generate any isotopy of 2-links in 4-space. Marked graphs can be represented by plane diagrams with small straight arcs denoting bridges over singular points, see Fig. 2, 9. In particular, the cyclic order of edges at each singular point is invariant.

Lemma 4.1 (Kauffman [8, Theorem 1, Figure 3 and Figure 9]) Marked graphs are isotopic in $\mathbb{R}^3$ if and only if their plane diagrams can be obtained from each other by finitely many Reidemeister moves in Fig. 13, where all symmetric images of the moves should be considered.

The moves in Fig. 13 are *local* in the sense, that a small disk in the left part of each move is replaced by another small disk in the right part of the move, while the rest of

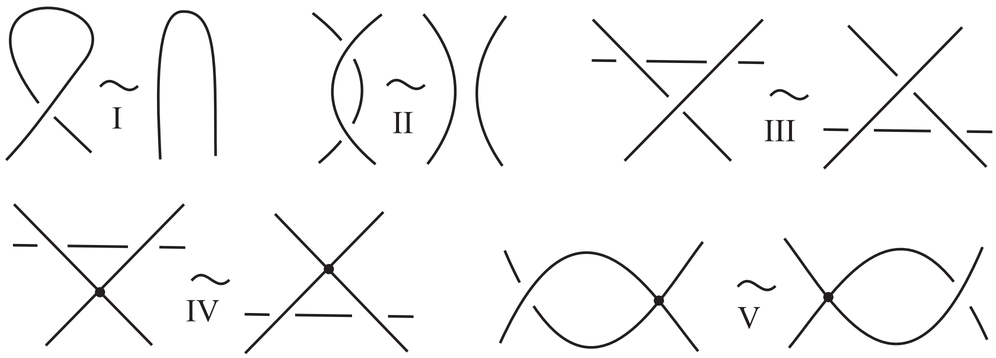

Figure 13: Reidemeister moves for rigid isotopy of marked graphs

the diagram remains unchanged. The singular points in moves IV and V of Fig. 13 can be equipped with arbitrary corresponding bridges. The proof is a direct application of the transversality theorem of Thom similarly to a proof of the Reidemeister theorem for plane diagrams of classical links, see analogous applications of singularity theory to links and graphs in Fiedler and Kurlin [5, section 2], [6, section 2].

Proposition 4.1 *Marked graphs represent isotopic 2-links in 4-space if and only if they can be obtained from each other by finitely many moves in Fig. 14*

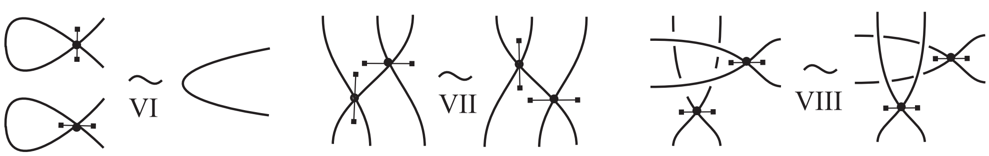

Figure 14: Moves of marked graphs generating isotopy of 2-links

Symmetric images of the moves in Fig. 14 are skipped as they can be reduced to the standard moves using an isotopy in $\mathbb{R}^3$. Proposition 4.1 was conjectured by K Yoshikawa in [15]. F Swenton [14] claimed a proof of Proposition 4.1 using banded links and the equivalent moves in Fig. 4. M Saito wrote in his review for the MathSciNet: 'It is claimed that this set of moves is equivalent to Yoshikawa's moves. It might be beneficial of some more detailed accounts, for example, those for the above claim, are discussed further and presented elsewhere in the literature'. The authors were asked by S Carter to fill in these details, so we give a more detailed proof of Proposition 4.1 for banded links. Recall that the singular subspace Σ of the space CS of 2-links was introduced in Definition 2.5. The following result will be formally deduced in 5 using the transversality theorem of Thom.

Claim 4.2 *(i) The closure of the subspace* Σ *has codimension 1 in the space* CS.

(ii) The complement of the closure $\overline{\Sigma}$ *in* CS *consists of generic 2-links.*

(iii) Any isotopy of 2-links can be deformed in such a way that all intermediate 2-links are generic apart from finitely many singularities of Definition 2.5.

(iv) If an isotopy passes through an A_2*-singularity, then a non-degenerate saddle and extremum collide and disappear as shown in the top picture of Fig. 18.*

Claims 4.2(i,ii) say that any point of CS can be removed from Σ by a small perturbation, i.e. a 2-link can be made generic, which implies Claim 2.3(ii). Claim 4.2(iii) says that the singularities of Definition 2.5 are the only singularities occuring in any isotopy of 2-links in general position.

Proof of Proposition 4.1 By Claim 4.2(iii) any isotopy of 2-links can be deformed into a smooth path transversal to the subspace $\Sigma \subset \mathrm{CS}$. When the path passes through one of the singularities, the associated banded link changes according to Proposition 2.6(iii),(iv), which led to the moves in Fig. 4 as required. □

4.2 A 1-dimensional encoding 2-links up to isotopy in 4-space

Here we reduce the isotopy classification of 2-links in 4-space to a word problem in the finitely presented semigroup SL, the universal semigroup of 2-links. Recall that moves (1–1)-(1–8) on 3-page embeddings were defined in subsection 1.3. Theorem 1.4 follows from the following generalisation of Lemma 3.3 to singular links.

Proposition 4.3 *(Kurlin and Vershinin [13]) Consider the semigroup* SK *generated by* a_i, b_i, c_i, d_i, x_i, $i \in \mathbb{Z}_3$*, subject to relations (1–1)-(1–5) from subsection 1.3. Then any singular link* $G \subset \mathbb{R}^3$ *is encoded by an element* $w_G \in \mathrm{SK}$ *in such a way that singular links* G, G' *are isotopic if and only if the elements* w_G *and* $w_{G'}$ *are equal in* SK*. An element* $w \in \mathrm{SK}$ *encodes a singular link if and only if* w *is central in* SK.

Proof of Theorem 1.4 Any 2-link can be represented by its marked graph G whose 3-page embedding is encoded by a word in the letters a_i, b_i, c_i, d_i, x_i, $i \in \mathbb{Z}_3$, as described before Proposition 3.2. All encoding elements form the centre of SL as the same result holds for the universal semigroup SK of singular links, i.e. relations (1–1)-(1–5) imply that any encoding element commutes with the generators.

The remaining part of Theorem thm:semigroup states that two 3-page embeddings of marked graphs represent isotopic 2-links in 4-space if and only if they can be related by algebraic moves (1–1)-(1–8) in subsection 1.3. By Lemmas 3.3, 3.4 and Proposition 4.1 it suffices to realise moves VI, VII, VIII in Fig. 14 by 3-page embeddings.

In moves VI, VII, VIII a small disk in the left part is replaced by another small disk in the right part. Similarly to the construction of a 3-page embedding, choose a path α passing through overcrossing arcs and bridges at singular points, see Fig. 15, 16, 17. Deform the diagrams in such a way that α becomes a straight line and push all overcrossing arcs into the half-plane P_1, all bridges remain in α.

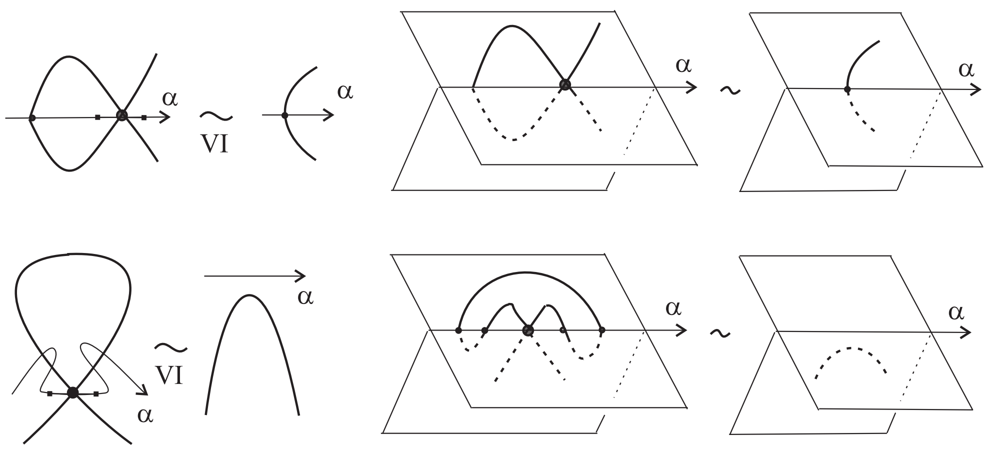

Figure 15: Realising moves VI of Fig. 14 in terms of 3-page embeddings

In Fig. 15 moves VI are encoded by $a_1x_1 = a_1$ and $a_1b_1x_1d_1c_1 = 1$ equivalent to (1–6) for $i = 1$. We made additional intersections of α with the diagram to decompose the resulting embedding into local 3-page embeddings from Fig. 7.

In Fig. 16 move VII is encoded by $d_1x_1b_1c_1x_1 = b_1x_1d_1c_1x_1$, which is (1–7) for $i = 1$. Numbers 1, 2, 3, 4, 5, 6 denote arcs going out of the small disk replaced by move VII, e.g. the path α starts between arcs 1, 4 and ends between arcs 3, 6.

In Fig. 17 move VIII is encoded by

$$(a_1b_1x_1b_1c_1)d_2d_1(b_2d_2)d_1d_0a_2b_2x_1b_1d_2b_1(b_2d_2)b_1b_2d_1^2 =$$

$$(a_1b_1x_1b_1c_1)b_0b_1(b_2d_2)a_1b_2a_2d_1(b_2d_2)d_1c_0b_1x_1b_1,$$

which is equivalent to (1–8) for $i = 1$ after removing $b_2d_2 = 1$ by relation (1–1). The relations for other $i \in \mathbb{Z}_3$ were added to make the presentation symmetric. □

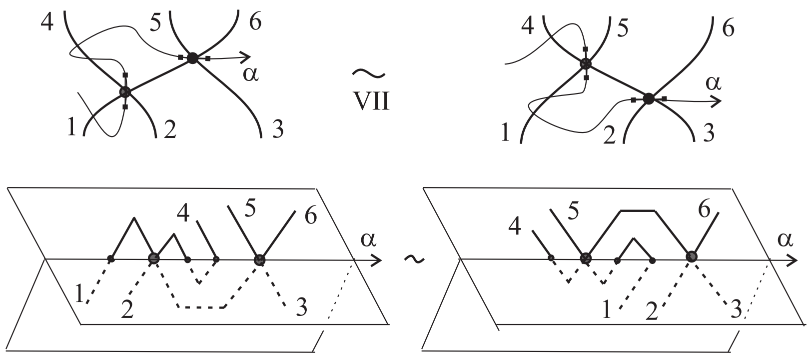

Figure 16: Realising move VII of Fig. 14 in terms of 3-page embeddings

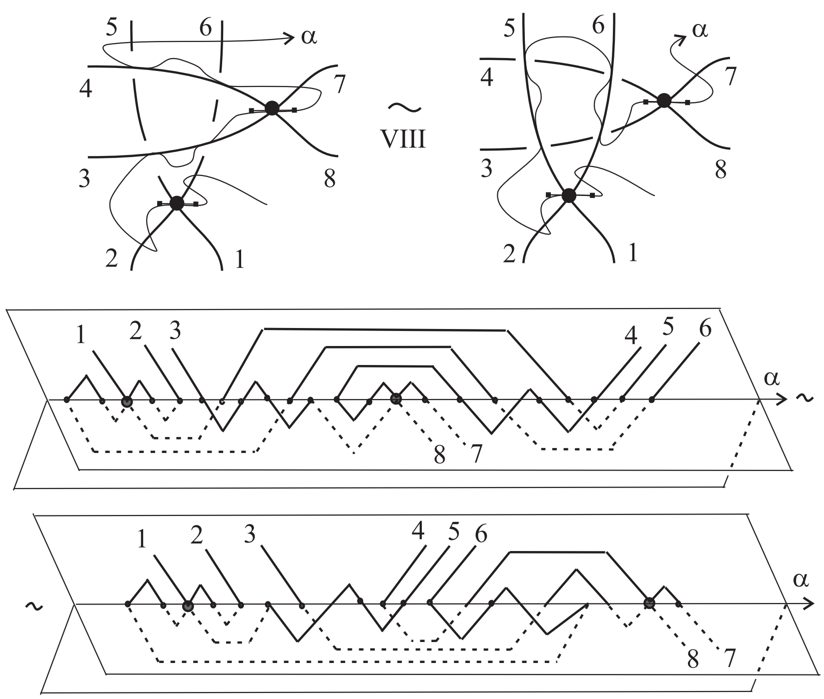

Figure 17: Realising move VIII of Fig. 14 in terms of 3-page embeddings

5 Appendix: the multi-jet transversality theorem of Thom

Here we follow Arnold, Varchenko and Gusein-Zade [1, sections I.2, I.8].

Let $\xi, \eta \colon M \to N$ be smooth maps between finite dimensional manifolds with Riemannian metrics ρ_M, ρ_N, respectively.

Definition 5.1 The maps ξ and η have the tangency of *order* k at a point $z \in M$ if k is the maximal integer such that $\rho_N(\xi(w), \eta(w))/(\rho_M(z,w))^k \to 0$ as $w \in M$ tends to z, e.g. the curve $\xi(w) = w^{k+1}$ has the tangency of order k with $\eta(w) = 0$.

The l-tuple k*-jet* of the map ξ at $(z_1, \dots, z_l) \in M^l$ is the equivalence class of smooth maps $\eta\colon M \to N$ up to tangency of order k at the points $z_1, \dots, z_l \in M$, e.g. the 1-tuple 1-jet $j^1_{[1]}\xi(z)$ of a map $\xi\colon \mathbb{R} \to \mathbb{R}$ is determined by $z, \xi(z), \dot{\xi}(z)$.

Denote by $J^k_{[l]}(M,N)$ the space of all l-tuple k-jets of smooth maps $\xi\colon M \to N$ for all $(z_1, \dots, z_l) \in M^l$. Let $(x_1, \dots, x_m)$ and $(y_1, \dots, y_n)$ be local coordinates in M and N, respectively. If ξ is defined locally by $y_j = \xi_j(x_1, \dots, x_m)$, $j = 1, \dots, n$, then the l-tuple k*-jet* of ξ at $(z_1, \dots, z_l)$ is determined by l arrays of the data below

$$\{x_1, \dots, x_m\}; \quad \{y_1, \dots, y_n\}; \quad \left\{\frac{\partial \xi_j}{\partial x_i}\right\}; \quad \dots \left\{\frac{\partial^k \xi_j}{\partial x_{i_1} \dots x_{i_s}}\right\}, i_1 + \dots + i_s = k.$$

The quantities above define local coordinates in $J^k_{[l]}(M,N)$. The l-tuple k*-jet* $j^k_{[l]}\xi$ of a smooth map $\xi\colon M \to N$ can be considered as the map $j^k_{[l]}\xi\colon M^l \to J^k_{[l]}(M,N)$, namely $(z_1, \dots, z_l)$ goes to the l-tuple k-jet of ξ at $(z_1, \dots, z_l)$.

The manifold $J^k_{[l]}(M,N)$ is finite dimensional, e.g. $J^0_{[l]}(M,N) = (M \times N)^l$,

$$\dim J^1_{[l]}(M,N) = (m+n+mn)l, \ \dim J^2_{[l]}(M,N) = (m+n+mn+\frac{m(m+1)}{2}n)l.$$

Definition 5.2 Take an open set $W \subset J^k_{[l]}(M,N)$. The set of smooth maps $f\colon M \to N$ with l-tuple k-jets from W is *open*. These sets for all open $W \subset J^k_{[l]}(M,N)$ over all k, l form a basis of the *Whitney* topology in $C^\infty(M,N)$. The space CS of all 2-links $S \subset \mathbb{R}^4$ inherits the *Whitney* topology from $C^\infty(S, \mathbb{R}^4)$.

So maps are close in the Whitney topology if they are close with all derivatives.

Definition 5.3 Let M be a finite dimensional smooth manifold. A subspace $\Lambda \subset M$ is called *a stratified space* if Λ is the union of disjoint smooth submanifolds Λ^i (*strata*) such that the boundary of each stratum is a finite union of strata of less dimensions. Let N be a finite dimensional manifold. A smooth map $\xi : M \to N$ is *transversal* to a smooth submanifold $U \subset N$ if the spaces $\xi_*(T_z M)$ and $T_{\xi(z)}U$ generate $T_{\xi(z)}N$ for each $z \in M$. A smooth map is $\eta : M \to V$ *transversal* to a stratified space $\Lambda \subset V$ if the the map η is transversal to each stratum of Λ.

Briefly Theorem 5.4 says that any map can be approximated by 'a nice map'.

Theorem 5.4 *(Multi-jet* transversality *theorem of Thom, see Arnold, Varchenko and Gusein-Zade [1, section I.2])*
Let M,N be compact smooth manifolds, $\Lambda\subset J^k_{[l]}(M,N)$ be a stratified space. Given a smooth map $\xi\colon\ M\to N$, there is a smooth map $\eta\colon\ M\to N$ such that

- *the map η is arbitrarily close to ξ with respect to the Whitney topology;*
- *the l-tuple k-jet $j^k_{[l]}\eta\colon\ M^l\to J^k_{[l]}(M,N)$ is transversal to $\Lambda\subset J^k_{[l]}(M,N)$.*

Proof of Claim 4.2 . (i) For any critical point of $\mathrm{pr}\colon\ S\to\mathbb{R}$, fix local coordinates $(x,y)\in S$ such that the derivatives $\mathrm{pr}_x=\mathrm{pr}_y=0$. The closures of the subspaces $\overline{\Sigma_{++}\cup\Sigma_{+-}\cup\Sigma_{--}}$ and $\bar\Sigma_2$ from Definition 2.5 can be mapped onto the subspaces of the finite-dimensional spaces $J^1_{[2]}(S,\mathbb{R})$ and $J^2_{[1]}(S,\mathbb{R})$ given by the equations $\mathrm{pr}(x_1,y_1)=\mathrm{pr}(x_2,y_2)$ and $\mathrm{pr}_{xx}\mathrm{pr}_{yy}-\mathrm{pr}^2_{xy}=0$, respectively. The resulting subspaces of jets have codimension 1 as preimages of 0 under smooth functions, e.g. the image of $\bar\Sigma_2$ in $J^2_{[1]}(S,\mathbb{R})$ is $(\mathrm{pr}_{xx}\mathrm{pr}_{yy}-\mathrm{pr}^2_{xy})^{-1}(0)$. Hence the closures $\overline{\Sigma_{++}\cup\Sigma_{+-}\cup\Sigma_{--}}$ and $\bar\Sigma_2$ have codimension 1 in the space CS of 2-links.

(ii) If a 2-link is not generic, then either some critical points of the projection $\mathrm{pr}\colon\ S\to\mathbb{R}$ are degenerate or have the same value. The singularities of Definition 2.5 are all multi local codimension 1 singularities of smooth functions $\mathbb{R}^2\to\mathbb{R}$, see Arnold, Varchenko and Gusein-Zade [1].

(iii) By Theorem 5.4 any smooth isotopy of 2-links is a path in CS and can be made transversal to the singular subspace $\bar\Sigma$, which has codimension 1 by (i), hence the new path will contain only finitely many isolated singularities of Definition 2.5.

(iv) The normal form of an A_2-singularity of a function $\mathbb{R}^2\to\mathbb{R}$ is $\mathrm{pr}(x,y)=x^2-y^3$, i.e. the projection $\mathrm{pr}\colon\ S\to\mathbb{R}$ has the form above in suitable local coordinates $(x,y)\in S$. A 2-link S, its cross-sections around the singularity and the graph of y^3 look like the middle pictures of Fig. 18. The versal deformation of an A_2-singularity is $\mathrm{pr}(x,y;\varepsilon)=x^2-y^3+\varepsilon y$, see Arnold, Varchenko and Gusein-Zade [1], i.e. any smooth deformation of $\mathrm{pr}(x,y)$ can be expressed as $f_1(x,y;\varepsilon)\cdot\mathrm{pr}(f_2(x,y;\varepsilon),f_3(x,y;\varepsilon);f_4(\varepsilon))$, where f_1,f_2,f_3,f_4 are smooth, $f_1(0,0;0)\neq 0$, $f_2(x,y;0)\equiv x$, $f_3(x,y;0)\equiv y$ and $f_4(0)=0$.

For $\varepsilon<0$, a 2-link S, its cross-sections around the singularity and the graph of $y^3-\varepsilon y$ look like the left pictures of Fig. 18. For $\varepsilon>0$, a 2-link S, its cross-sections around

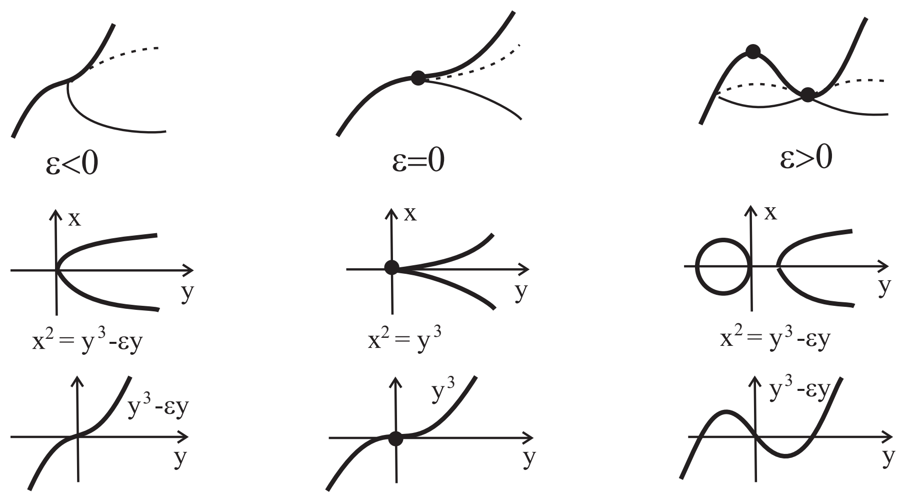

Figure 18: Transformation of a 2-link near an A_2-singularity

the singularity and the graph of $y^3 - \varepsilon y$ look like the right pictures of Fig. 18. For instance, 2-links for $\varepsilon > 0$ have a non-degenerate saddle at $x = 0$, $y = \sqrt{\varepsilon/3}$ and a local extremum at $x = 0$, $y = -\sqrt{\varepsilon/3}$. □

References

[1] V Arnold, A Varchenko, S Gusein-Zade, Singularities of Differentiable Maps, Moscow, 1982.

[2] S Carter, M Saito, Knotted Surfaces and Their Diagrams, Math. Surveys and Monographs, v. 55, Providence, R.I. : Amer. Math. Soc., 1998.

[3] I Dynnikov, Three-page approach to knot theory. Encoding and local moves, Functional Analysis and Its Applications 33 (1999), 260–269.

[4] I Dynnikov, Three-page approach to knot theory. Universal semigroup, Functional Analysis and Its Applications 34 (2000), 24–32.

[5] T Fiedler, V Kurlin, A one-parameter approach to links in solid torus, arXiv: math.GT/0606381.

[6] T Fiedler, V Kurlin, Fiber quadrisecants in knot isotopies, arXiv: math.GT/0701878, to appear in J Knot Theory Ramifications 17 (2008).

[7] R Fox, J Milnor, Singularities of 2-spheres in 4-space and cobordism of knots, Osaka J. Math. **3** (1966), 257–267.

[8] L Kauffman, Invariants of Graphs in Three-Space, Trans. Amer. Math. Soc., **311** (1989), no. 2, 697–710.

[9] A Kawauchi, A survey of knot theory, Birkhauser Verlag (1996).

[10] A Kawauchi, T T Shibuya, S Suzuki, Description of surfaces in 4-space.I.Normal forms, Math. Sem. Notes Kobe Univ., **10** (1982), 75–125.

[11] C Kearton, W B R Lickorish, Piecewise linear critical levels and collapsing, Trans. Amer. Math. Soc., **170** (1972), 415–424.

[12] V Kurlin, Three-page encoding and complexity theory for spatial graphs, J. Knot Theory Ramifications **16** (2007), no. 1, 59–102.

[13] V Kurlin, V Vershinin, Three-page embeddings of singular knots, Functional Anal. Appl. **35** (2004), no. 1, 14–27.

[14] F Swenton, On a calculus for 2-knots and surfaces in 4-space, J. Knot Theory Ramif. **10** (2001), no. 8, 1133–1141.

[15] K Yoshikawa, An enumeration of surfaces in 4-space, Osaka J. Math. **31** (1994), 497–522.

Department of Mathematical Sciences,, Durham University, Durham DH1 3LE, United Kingdom

Department of Mathematical Sciences,, Durham University, Durham DH1 3LE, United Kingdom

cherry.kearton@durham.ac.uk, vitaliy.kurlin@durham.ac.uk

http://www.maths.dur.ac.uk/~dma0ck/, http://maths.dur.ac.uk/~dma0vk/

Received: 7 April 2008 Revised: 7 June 2008